The role of the environment time scale in light-harvesting efficiency and coherent oscillations

2012 New J. Phys. 14 073027

(http://iopscience.iop.org/1367-2630/14/7/073027)

New Journal of Physics
The open-access journal for physics

The role of the environment time scale in light-harvesting efficiency and coherent oscillations

Arend G Dijkstra and Yoshitaka Tanimura
Department of Chemistry, Graduate School of Science, Kyoto University, Kyoto 606-8502, Japan
E-mail: dijkstra@kuchem.kyoto-u.ac.jp and tanimura@kuchem.kyoto-u.ac.jp

New Journal of Physics **14** (2012) 073027 (11pp)
Received 26 April 2012
Published 12 July 2012
Online at http://www.njp.org/
doi:10.1088/1367-2630/14/7/073027

Abstract. We study the efficiency of exciton transport as a function of the typical reorganization time scale of the environment using the hierarchy of equations of motion. As a model system, we choose the Fenna–Matthews–Olson (FMO) complex. An environment in which the dynamics is not much faster than the system leads to prolonged quantum coherent transport, even at room temperature. We find that this does not make the transport process more efficient for standard FMO parameters, but does increase the efficiency in the case when exciton decay competes with trapping at the reaction center. We furthermore find that initial correlations do not influence population oscillations.

Contents

1. Introduction

Photosynthesis provides a biological model for efficiently harvesting the light of the sun [1]. Captured sunlight is transferred in the form of electronic excitations from antenna molecules to a reaction center, where it can be used. The mechanism of the light-harvesting process and, in particular, the parameters that determine its efficiency are subjects of fundamental interest, but are also relevant to future technology. How can energy be transported efficiently in a complex biological system at room temperature?

Energy in light-harvesting systems is transferred between chromophore molecules. The flow of energy can occur because the electronic excited states on these chromophores are coupled. If these couplings are strong, energy can flow coherently, as a quantum mechanical wave. On the other hand, noise induced by the protein and water environment interferes with wave-like motion and leads to decoherence and classical hopping. In complex systems at high temperature, the noise is expected to be strong and may be the dominant effect. Coherent energy flow is hardly expected because of the strong decoherence in this situation. However, recent experimental studies using nonlinear optical spectroscopy have found evidence for quantum coherent motion in biological light-harvesting complexes [2–4]. In addition, theoretical calculations have shown that quantum coherence can be sustained for several hundreds of femtoseconds, the same time scale on which energy transport takes place [5].

Even if electronic coherence and not coupling to vibrations [6–10] is observed in light-harvesting complexes, it is not clear whether coherent transport is important for the efficiency of the harvesting mechanism. If so, what are the parameters to be optimized in artificial systems that improve the role of coherent transport? The efficiency of energy transfer and, in particular, the role of quantum coherence have been a topic given much theoretical attention [11–17]. It was found that the interplay of coherent dynamics and environmental noise leads to optimal energy transfer [12, 13, 18–20].

These previous studies have used the Haken–Strobl model or the Lindblad or Redfield equations to model the dynamics. The underlying approximation of a fast environment, however, breaks down in the case of light-harvesting complexes, where the time scale of the environment is comparable to that of the system dynamics [21]. Ishizaki and Fleming [22] showed that a proper treatment of the time scale of the environment leads to prolonged coherent oscillations. These oscillations were calculated to be present in the FMO complex for up to 400 femtoseconds at room temperature [5]. A proper theory of exciton dynamics in the FMO complex should include these memory effects inherent in a slower environment and cannot use the Redfield, Lindblad or Haken–Strobl models.

The slow dynamics in the environment, which takes place on the same time scale as the relaxation in the system, is thus responsible for prolonged oscillations in the site populations. What is not clear, however, is whether this effect also improves the light-harvesting process. In this paper, we study the effect of the time scale of the environment on the light-harvesting efficiency, without making the fast bath (Markovian) approximation. To this end, we use the hierarchy of equations of motion for the reduced density operator [22–30]. We will compare a fast environment, where the Markovian limit is valid and coherent oscillations are absent, with an environment that evolves on similar time scales as the system dynamics and investigate whether the light-harvesting efficiency is different in both cases.

The coherent oscillations in biological light-harvesting complexes were observed experimentally using the technique of two-dimensional (2D) optical spectroscopy. In these

experiments, three short laser pulses separated by controllable time intervals t_1, t_2 and t_3 interact with the sample. Exciton transport and possible coherent oscillations of exciton populations are observed during the waiting time t_2. Crucially, at the beginning of the waiting time, exciton population is not simply created by optical excitation from the ground state. Rather, the system has already evolved during the time t_1 in a coherent superposition of the ground state and the exciton states. During this coherence time, correlations between the chromophore system and the environment build up, which can influence the exciton dynamics during t_2. That such correlations, which lead to memory effects, are indeed present is clear from the observed line shape in the 2D spectra [2]. The spectral line shape that, simply stated, correlates the state of the system during t_1 with its state during t_3 clearly shows these memory effects. We therefore ask the question of whether initial correlations between the system and the environment, created during t_1, influence the observed coherent oscillations during t_2.

Such a study of exciton populations must include correlations between the system and the environment present at the moment of interaction with the external laser pulse. Such correlations are neglected in master equations, which are therefore not suitable to study the role of initial correlations. Suitable methods for the simulation of 2D spectra include numerical integration of the Schrödinger equation and the hierarchy of equations of motion. Using these methods, 2D spectra of the FMO complex have been simulated [31–34]. We will use the hierarchy of equations of motion, which allows proper treatment of these correlations to answer the question of whether population oscillations during t_2 depend on correlations between the system and the environment created during t_1.

The remainder of this paper is organized as follows. In section 2, we introduce our theoretical model. In section 3, we calculate the excitation dynamics and show the results for the light-harvesting efficiency as a function of the time scale of the environment. In section 4, we investigate the effect of initial correlations as created in a nonlinear optical experiment on the exciton dynamics. We present our conclusions in section 5.

2. The model

The light-harvesting system consists of N chromophores, which we model with the usual Frenkel exciton Hamiltonian. It is written in terms of the creation and annihilation operators $c_n^\dagger$ and c_n for the chromophores, labeled with indices n and m, which run from 1 to N, as

$$H_S = \sum_n \epsilon_n c_n^\dagger c_n + \sum_{nm} J_{nm} c_n^\dagger c_m. \tag{1}$$

The parameters ϵ_n are the excitation energies of site n, while J_{nm} denotes the coherent coupling between sites n and m. Several models exist for these quantities [35, 36]. Here, we will use the following Hamiltonian in the one-quantum site representation [35]:

$$H_S = \begin{pmatrix} 280 & -106 & 8 & -5 & 6 & -8 & -4 \\ -106 & 420 & 28 & 6 & 2 & 13 & 1 \\ 8 & 28 & 0 & -62 & -1 & -9 & 17 \\ -5 & 6 & -62 & 175 & -70 & -19 & -57 \\ 6 & 2 & -1 & -70 & 320 & 40 & -2 \\ -8 & 13 & -9 & -19 & 40 & 360 & 32 \\ -4 & 1 & 17 & -57 & -2 & 32 & 260 \end{pmatrix}. \tag{2}$$

Note that there is recent evidence for an eighth chromophore in the FMO complex [37, 38], which is not included in our current calculation. It was found that the seven- and eight-site models display similar energy transport efficiencies [38].

In addition to the coherent dynamics described by this Hamiltonian, the system is subject to incoherent decay and trapping processes [19]. Decay is the irreversible loss of exciton populations due to radiative and non-radiative processes in each chromophore, whereas trapping is the desired loss of population due to hopping to the reaction center. Including these processes, the Liouville operator is written as

$$L_S = \hat{H}_S^{\times} + L^{(\mathrm{decay})} + L^{(\mathrm{trap})}, \tag{3}$$

where $\hat{A}^{\times}B = [A, B]$ denotes the commutator and $L^{(\mathrm{decay})}$ and $L^{(\mathrm{trap})}$ model the decay and trapping processes. We will assume that the exciton decay rate is independent of the chromophore and proceeds with a rate $k^{(\mathrm{decay})}$, $L^{(\mathrm{decay})}_{nmn'm'} = -k^{(\mathrm{decay})}$. Trapping occurs only on site 3 with a rate $k^{(\mathrm{trap})}$, $L^{(\mathrm{decay})}_{nmnm} = -\frac{k^{(\mathrm{trap})}}{2}(\delta_{n3} + \delta_{m3})$.

In order to model decoherence each chromophore is coupled to an independent bath of harmonic oscillators, which is described by the Hamiltonian

$$H_{\mathrm{B}} = \sum_{\alpha} \left(\frac{p_\alpha^2}{2m_\alpha} + \frac{1}{2} m_\alpha \omega_\alpha^2 x_\alpha^2 \right). \tag{4}$$

The coupling is taken to be linear in the coordinates of the harmonic oscillators as

$$H_{\mathrm{SB}} = -\sum_{n\alpha} g_{n\alpha} c_n^{\dagger} c_n x_\alpha. \tag{5}$$

All the necessary information about the bath and the system–bath coupling is encoded in the spectral densities, which give the density of bath states weighed by their coupling to the system. They are given by

$$\mathcal{J}_n(\omega) = \sum_{\alpha} \frac{g_{n\alpha}^2}{2m_\alpha \omega_\alpha} \delta(\omega - \omega_\alpha). \tag{6}$$

We assume that each chromophore couples to an independent bath, that is, that no correlations between the fluctuations in different chromophore energies are present. We furthermore assume that all baths are equal, so that the spectral densities $\mathcal{J}_n$ have the same functional form for each n, which we will denote as $\mathcal{J}(\omega)$. A practical choice for the spectral densities is given by the Drude model. The Drude spectral density is given by

$$\mathcal{J}(\omega) = 2\lambda \frac{\omega\gamma}{\gamma^2 + \omega^2}. \tag{7}$$

In this model, the bath is represented by a single time scale $\tau = 1/\gamma$. The hierarchy approach that we will use is not limited to this spectral density, but has been extended to treat a Brownian spectral distribution [39, 40] and, recently, to more general spectral densities [41].

In the Drude case, and assuming the high temperature limit ($\beta\hbar\gamma < 1$, where β is the inverse temperature), the correlation functions for the effective bath modes are given by [23, 25]

$$C(t) = c\, \mathrm{e}^{-\gamma|t|}, \tag{8}$$

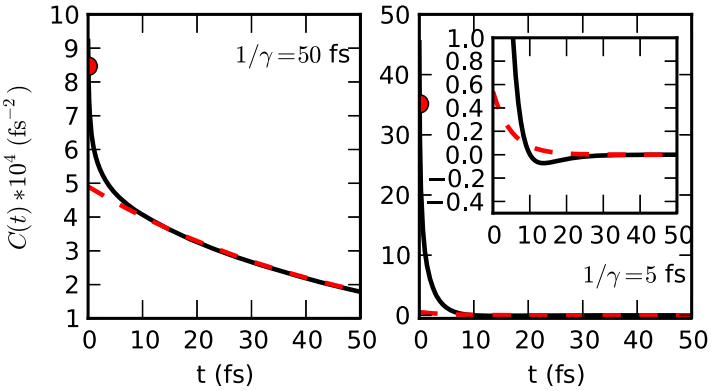

Figure 1. Correlation functions (solid) and the approximated form used in our calculations (dashed) for a bath timescale of (left) 50 fs and (right) 5 fs.

with the prefactor

$$c = \lambda \left(-\mathrm{i}\gamma + \frac{2}{\beta} \right). \tag{9}$$

The real part of the correlation function describes the fluctuations induced in the chromophore transition energy by the interaction with the bath. The imaginary part is responsible for dissipation of energy.

In the high temperature approximation, the hierarchy of equations of motion is given by

$$\dot{\rho}^{\{p\}}(t) = -\left(\mathrm{i}L_S + \sum_n p_n \gamma \right) \rho^{\{p\}}(t) - \mathrm{i} \sum_n p_n \left(c V_n \rho^{p_n^-} - c^* \rho^{p_n^-} V_n \right) - \mathrm{i} \sum_n \hat{V}_n^{\times} \rho^{p_n^+}. \tag{10}$$

The object that is propagated in time is a hierarchy of density matrices, which are labeled by a set of N indices, denoted as $\{p_n\}$. The matrix with all indices equal to zero is the physical reduced density matrix for the chromophore system, whereas the other matrices are auxiliary density matrices that account for memory stored in the bath. The notation $\rho^{p_n^-}$ and $\rho^{p_n^+}$ refers to a decrease or increase of the nth index by one. With little extra computational cost, the hierarchy can be extended by approximately including low-temperature correction terms [26, 42] as described by Ishizaki and Fleming [5]. The equations of motion with low-temperature correction terms, similar to equation (10), will be used for the computations in this paper. Figure 1 shows the correlation function and the approximation used in the calculations in this paper. The approximation is excellent for the physical bath timescale of 50 fs. For the case of 5 fs, the approximation misses the very small negative part of the correlation function, and is very small apart from the delta-function contribution at zero time. In this case, our calculation is essentially done in the Markovian approximation. The hierarchy can be propagated in time to give the exciton populations and coherences. In the absence of exciton decay and trapping, a steady state will be reached. We mention that this steady state is not equal to the Boltzmann distribution with respect to the system Hamiltonian only, because of the coupling to a bath. However, in our calculations exciton decay and trapping are present and no steady state is reached.

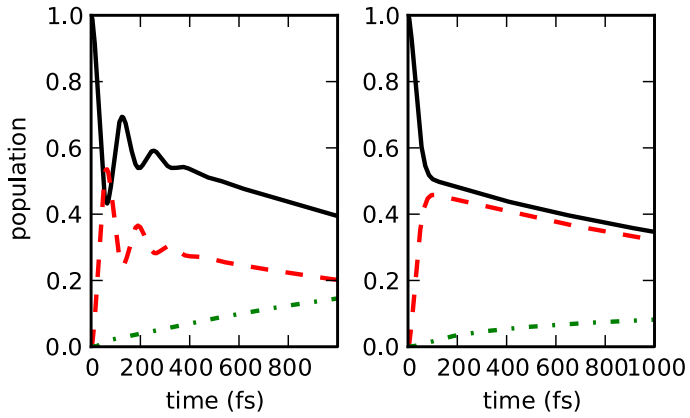

Figure 2. Population on (solid line) chromophore 1, (dashed line) 2 and (dash-dotted line) 3 for (left) $\tau = 50\,\text{fs}$ and (right) $\tau = 5\,\text{fs}$. The reorganization energy is $\lambda = 35\,\text{cm}^{-1}$ and the temperature is $T = 300\,\text{K}$.

3. Light-harvesting efficiency

The efficiency of the light-harvesting process can be calculated from the competition between the trapping and decay processes. The total time an excitation spends on site n is given by

$$\tau_n = \int_0^\infty \mathrm{d}t \rho_{nn}(t). \tag{11}$$

The efficiency can then be calculated as [14, 19]

$$E = \frac{k_3^{(\text{trap})}}{k_3^{(\text{trap})} + \sum_n k_n^{(\text{decay})} \tau_n}. \tag{12}$$

We are now in a position to discuss the question of how the time scale of the environment $\tau = 1/\gamma$ influences the light-harvesting efficiency and whether quantum coherence plays an important role. To that end, we first consider the population dynamics after initial excitation of chromophore one, which, together with the newly discovered chromophore eight, forms the entrance route for excitation energy [37]. Figure 2 shows the early time dynamics. The key effect that leads to prolonged quantum oscillations is the time scale of the environment. For a time scale $\tau = 1/\gamma = 50\,\text{fs}$, clear oscillations in the populations are visible for times up to 400 fs. For a much faster environment with $\tau = 5\,\text{fs}$, the oscillations disappear and the dynamics appears to be completely incoherent. Other parameters were set to $\lambda = 35\,\text{cm}^{-1}$ for the reorganization energy and $T = 300\,\text{K}$ as the temperature. The time scale of 5 fs was chosen only for comparison and is not realistic in the case of light-harvesting complexes. Calculation of the exciton dynamics for this parameter value is, however, useful in studying the effect of the presence or absence of coherent oscillations.

For the light-harvesting process, however, the longer time scale dynamics are much more important. Does the existence of coherent oscillations in the populations in the first few 100 fs really improve the light-harvesting process? To answer this question, we plot the dynamics for a longer time in figure 3. Surprisingly, the time scale of the bath is not only important at short times, but also strongly affects the dynamics at longer times. Crucially, the population on chromophore 3 for a bath time scale of $\tau = 50\,\text{fs}$ is of the order of two times larger than that for

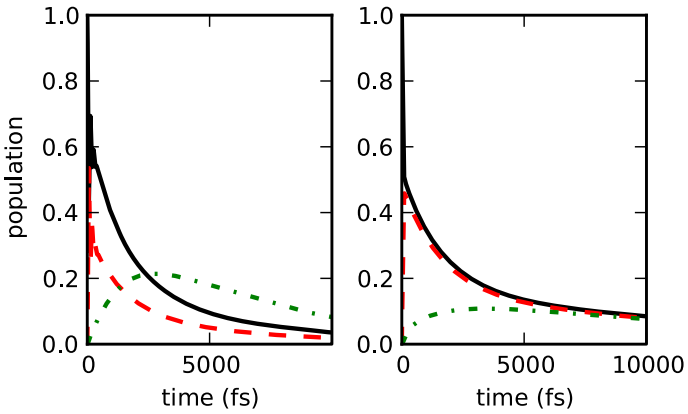

Figure 3. Population on (solid line) chromophore 1, (dashed line) 2 and (dash-dotted line) 3 for (left) $\tau = 50$ fs and (right) $\tau = 5$ fs. The reorganization energy is $\lambda = 35\,\mathrm{cm}^{-1}$ and the temperature is $T = 300$ K.

the case of 5 fs. This population is, in particular, important because chromophore 3 is connected to the reaction center, and thus energy is trapped from this site.

The efficiency of the light-harvesting process can be calculated directly from equation (12). To apply this equation, we run trajectories of the dynamics for 100 ps and then use equation (12) to calculate the efficiency. The decay and trapping times were chosen to be $1/k^{(\mathrm{decay})} = 1$ ns and $1/k^{(\mathrm{trap})} = 1$ ps, respectively [19]. For the previously discussed cases of $\tau = 50$ fs and $\tau = 5$ fs, the efficiencies are $E = 99.6$ percent and $E = 99.24$ percent, respectively. We see that, although the dynamics is significantly different, the efficiency is almost the same in both cases. Although a slower environment allows the excitation to explore the chromophore system coherently and thus leads to fundamentally different dynamics, the effect on efficiency is small. This is caused by the decay rate being so much smaller than the trapping rate. As a result, the population always reaches the trap before it can decay, albeit more slowly.

To show that the result that the environment time scale, and thus the presence of quantum coherence, does not influence the light-harvesting efficiency is indeed a consequence of the slow decay time, we varied this decay time. We repeated our calculation with a decay time of $1/k^{(\mathrm{decay})} = 10$ ps, and found efficiencies of 72% for a 50 fs environment and 55% for a 5 fs environment. In this case, exciton trapping really competes with exciton decay. A slower environment, which enables more coherent movement of the excitation through the complex, enables more efficient light harvesting. This finding may be relevant for artificial light-harvesting systems, and shows that to understand the effect of quantum coherence on efficiency it is necessary to repeat the calculations with parameters relevant to the system under study.

Because this significantly increased efficiency is an interesting result not only from the viewpoint of FMO, but also for the design of artificial light-harvesting systems, we study this case a little more. With a 10 ps exciton decay time, the population dynamics looks similar to the 1 ns case shown in figures 2 and 3 (data not shown). Again, we find that a slower environment leads to more population being transferred to site 3, where trapping takes place. The light-harvesting efficiency as a function of the bath time scale is shown in figure 4. We find a maximum efficiency between 50 and 100 fs, which is precisely the range expected in natural light-harvesting [36, 43]. We conclude that the time scale of the environment and, thus, the

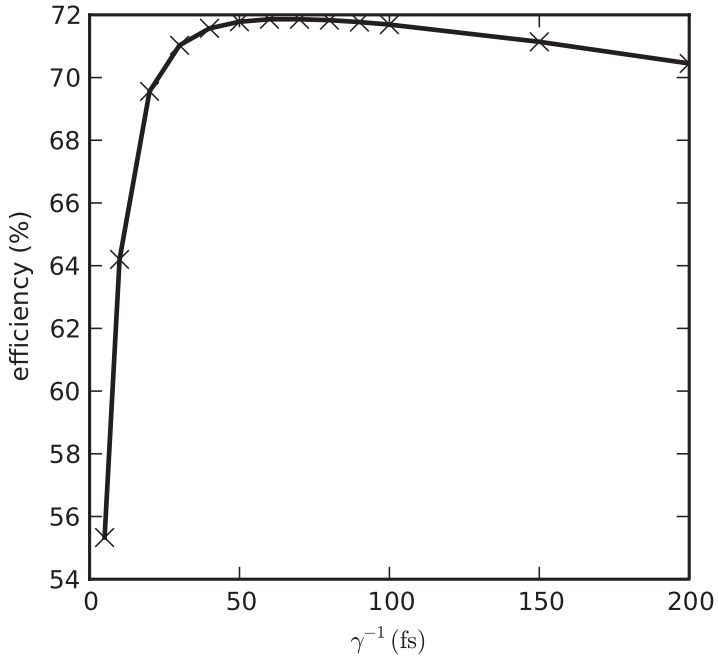

Figure 4. Light-harvesting efficiency as a function of the typical timescale of the bath. The reorganization energy is $\lambda = 35\,\mathrm{cm}^{-1}$ and the temperature is $T = 300\,\mathrm{K}$. The exciton decay time is $\tau^{\mathrm{decay}} = 10\,\mathrm{ps}$.

presence of quantum coherence are important for the light-harvesting efficiency if exciton decay competes with trapping at the reaction center.

4. Initial correlations

The time evolution of the populations as shown in figures 2 and 3 was calculated by assuming an artificial initial condition. In this section, we look at a model that is closer to the experimental case. In a 2D experiment, exciton population is followed as a function of a waiting time t_2. The system is excited by two ultrashort laser pulses, separated by a coherence time t_1, and the waiting time starts after pulse two. There are two differences to the artificial initial condition chosen before. First of all, the laser light excites not only a single chromophore, but all of them simultaneously, according to their transition dipole to the ground state. This initial condition can be simulated by simply choosing this as the initial condition for the simulation. In our calculations, we will assume that the transition dipoles are the same for each chromophore [32], and neglect the effects of laser polarization.

The second effect of the experimental initial condition is much more serious. During the coherence time t_1, correlations between the chromophores and the bath build up. Therefore, at the beginning of t_2, the chromophore system and the bath are not independent. We include these correlations in our calculation by explicitly simulating the dynamics as a function of t_1 and t_2 for a specific (photon echo) excitation sequence. The quantity that we calculate is

$$S(t_1, t_2) = G(t_1 + t_2; t_1)(\mu G(t_1; 0)(\rho(0)\mu)), \tag{13}$$

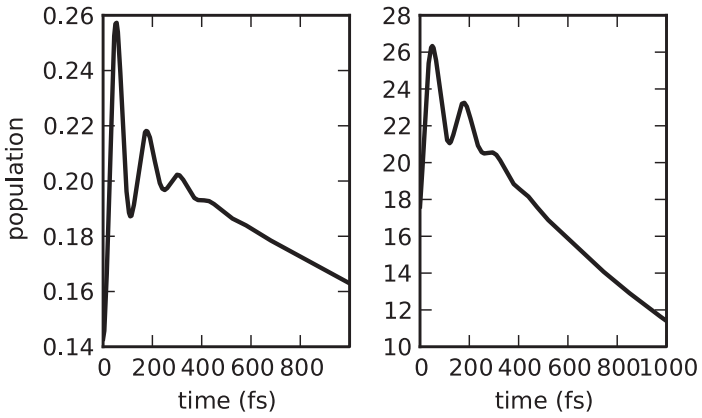

Figure 5. Response function as a function of t_2 for (left) zero t_1 and (right) $t_1 = 500$ fs.

where μ is the transition dipole operator and G is the free propagation of the system as well as the bath. The propagators G are the solution of $\rho(t) = G(t; t_0)\rho(t_0)$ and are evaluated by propagating the hierarchy of equations of motion. By varying t_1, we can include initial correlations between the chromophore system and the bath to varying extent. For $t_1 = 0$, no such correlations are present, while they are allowed to form for nonzero t_1. Note that the calculated populations are not directly observable in experiment.

As seen from figure 5, which shows the response function as a function of t_2 for two values of t_1, there is almost no effect of the initial correlations on the duration of the oscillations during the waiting time. This means that a simple calculation of populations as a function of time is sufficient to understand the data obtained in nonlinear optical experiments when one is interested in the persistence of coherent oscillations. There is, however, a quantitative difference between the two lines in figure 5. For a detailed understanding of the data it is therefore necessary to simulate the nonlinear experiment, which allows for a direct comparison with experiment.

5. Conclusion

In conclusion, we studied the light-harvesting efficiency in the FMO complex using the hierarchy of equations of motion as a function of the time scale of the environment. For an environmental time scale of the same order as the time scale of the system, as expected for biological light-harvesting complexes, coherent oscillations are present in the exciton populations for the first few hundreds of femtoseconds. For a shorter environmental timescale, these oscillations are suppressed and the dynamics appears to be incoherent. We find that the presence of coherence also influences the population transfer on a longer timescale. However, using values from the literature for the exciton decay and trapping processes, we find that the presence of quantum coherence is not important for the light-harvesting efficiency in the FMO complex. However, if exciton decay is fast enough to compete with the trapping process, coherence does help to reach the trap and the efficiency increases in the presence of coherence.

In 2D spectroscopy, a tool used to investigate quantum coherence in biological systems experimentally, population dynamics is observed during the waiting time t_2. This time interval is preceded by a coherence time t_1, during which correlations between the chromophore

system and the environment can be formed [44, 45]. We investigated the effect of these initial correlations on the population dynamics and found no significant difference in the lifetime of the coherent oscillations.

Acknowledgment

AGD acknowledges the Japan Society for the Promotion of Science for support in the form of a postdoctoral fellowship for foreign researchers.

References

[1] Scholes G D, Fleming G R, Olaya-Castro A and van Grondelle R 2011 *Nature Chem.* **3** 763
[2] Engel G S, Calhoun T R, Read E L, Ahn T-K, Mančal T , Cheng Y-C, Blankenship R E and Fleming G R 2007 *Nature* **446** 782
[3] Collini A, Wong C Y, Wilk K E, Curmi P M G, Brumer P and Scholes G D 2010 *Nature* **463** 644
[4] Panitchayangkoon G, Voronine D V, Abramavicius D, Caram J R, Lewis N H C, Mukamel S and Engel G S 2011 *Proc. Natl Acad. Sci. USA* **108** 20908
[5] Ishizaki A and Fleming G R 2009 *Proc. Natl Acad. Sci. USA* **106** 17255
[6] Christensson N, Kauffmann H F, Pullerits T and Mančal T 2012 *J. Phys. Chem.* **116** 7449
[7] Olšina J and Mančal T 2012 *J. Chem. Phys.* doi:10.1016/j.chemphys.2012.02.022
[8] Olbrich C, Strümpfer J, Schulten K and Kleinekathöfer U 2011 *J. Phys. Chem. Lett.* **2** 1771
[9] Nalbach P, Braun D and Thorwart M 2011 *Phys. Rev.* E **84** 041926
[10] Rätsep M and Freiberg A 2007 *J. Lumin.* **127** 251
[11] Olaya-Castro A, Lee C F, Olsen F F and Johnson N F 2008 *Phys. Rev.* B **78** 085115
[12] Mohseni M, Rebentrost P, Lloyd S and Aspuru-Guzik A 2008 *J. Chem. Phys.* **129** 174106
[13] Caruso F, Chin A W, Datta A, Huelga S F and Plenio M B 2009 *J. Chem. Phys.* **131** 105106
[14] Vlaming S M and Silbey R J 2012 arXiv:1111.3627v1
[15] Wu N, Sun K-W, Chang Z and Zhao Y 2012 *J. Chem. Phys.* **136** 124513
[16] Wang H B, Pshenichnyuk I, Hartle R and Thoss M 2011 *J. Chem. Phys.* **135** 244506
[17] Wu J, Liu F, Ma J, Silbey R J and Cao J 2011 arXiv:1109.5769v1
[18] Plenio M B and Huelga S F 2008 *New J. Phys.* **10** 113019
[19] Wu J, Liu F, Shen Y, Cao J and Silbey R J 2010 *New J. Phys.* **12** 105012
[20] Kassal I and Aspuru-Guzik A 2012 arXiv:1201.5202v1
[21] Ishizaki A and Fleming G R 2009 *J. Chem. Phys.* **130** 234110
[22] Ishizaki A and Fleming G R 2009 *J. Chem. Phys.* **130** 234111
[23] Tanimura Y and Kubo R 1989 *J. Phys. Soc. Japan* **58** 101
[24] Ishizaki A and Tanimura Y 2005 *J. Phys. Soc. Japan* **74** 3131
[25] Tanimura Y 2006 *J. Phys. Soc. Japan* **75** 082001
[26] Ishizaki A and Tanimura Y 2007 *J. Phys. Chem.* A **111** 9269
[27] Strümpfer J and Schulten K 2009 *J. Chem. Phys.* **131** 225101
[28] Chen L, Zheng R, Shi Q and Yan Y 2009 *J. Chem. Phys.* **131** 094502
[29] Dijkstra A G and Tanimura Y 2010 *Phys. Rev. Lett.* **104** 250401
[30] Kreisbeck C, Kramer T, Rodríguez M and Hein B 2011 *J. Chem. Theory Comput.* **7** 2166
[31] Sharp L Z, Egorova D and Domcke W 2010 *J. Chem. Phys.* **132** 014501
[32] Chen L, Zheng R, Jing Y and Shi Q 2011 *J. Chem. Phys.* **134** 194508
[33] Olbrich C, Tl Jansen C, Liebers J, Aghtar M, Strümpfer J, Schulten K, Knoester J and Kleinekathöfer U 2011 *J. Phys. Chem.* B **115** 8609
[34] Hein B, Kreisbeck C, Kramer T and Rodríguez M 2012 *New J. Phys.* **14** 023018

[35] Vulto S I E, de Baat M A, Louwe R J W, Permentier H P, Neef T, Miller M, van Amerongen H and Aartsma T J 1998 *J. Phys. Chem.* B **102** 9577
[36] Adolphs J and Renger T 2006 *Biophys. J.* **91** 2778
[37] Schmidt am Busch M, Müh F, El-Amine Madjet M and Th Renger 2011 *J. Phys. Chem. Lett.* **2** 93
[38] Moix J, Wu J, Huo P, Coker D and Cao J 2011 *J. Phys. Chem. Lett.* **2** 3045
[39] Tanimura Y and Mukamel S 1994 *J. Phys. Soc. Japan* **63** 66
[40] Tanaka M and Tanimura Y 2009 *J. Phys. Soc. Japan* **78** 073802
[41] Kreisbeck C and Kramer T 2012 arXiv:1203.1485v1
[42] Tanimura Y 1990 *Phys. Rev.* A **41** 6676
[43] Cho M, Vaswani H M, Brixner T, Stenger J and Fleming G R 2005 *J. Phys. Chem.* B **109** 10542
[44] Dijkstra A G and Tanimura Y 2012 *Phil. Trans. R. Soc.* A **370** 3658
[45] Dijkstra A G and Tanimura Y 2012 *J. Phys. Soc. Japan* **81** 063301